Discrete Models for Seismic Analysis of Liquid Storage Tanks of Arbitrary Shape and Fill Height

G. C. Drosos

A. A. Dimas[1]
e-mail: adimas@upatras.gr

D. L. Karabalis

Department of Civil Engineering,
University of Patras,
26500 Patras, Greece

A finite element method (FEM)-based formulation is developed for an effective computation of the eigenmode frequencies, the decomposition of total liquid mass into impulsive and convective parts, and the distribution of wall pressures due to sloshing in liquid storage tanks of arbitrary shape and fill height. The fluid motion is considered to be inviscid (slip wall condition) and linear (small free-surface steepness). The natural modal frequencies and shapes of the sloshing modes are computed, as a function of the tank fill height, on the basis of a conventional FEM modeling. These results form the basis for a convective-impulsive decomposition of the total liquid mass, at any fill height, for the first few (two or three at most) sloshing modes, which are by far the most important ones in comparison to all other higher modes. This results into a simple yet accurate and robust model of discrete masses and springs for the sloshing behavior. The methodology is validated through comparison studies involving vertical cylindrical tanks. Additionally, the application of the proposed methodology to conical tanks and to the seismic analysis of spherical tanks on a rigid or flexible supporting system is demonstrated and the results are compared to those obtained by rigorous FEM analyses. [DOI: 10.1115/1.2967834]

1 Introduction

Although the early interest on the dynamic characteristics of a contained liquid dates back to the beginning of the previous century, e.g., Ref. [1], the 1964 Alaska earthquake and the extensive damage it inflicted on various kinds of liquid storage tanks seems to have initiated an intense and uninterrupted, since then, interest on the seismic behavior of modern structures used for the storage of liquids or liquidlike materials, e.g., water, fuel, oil products, chemicals, wastes, and liquefied natural gas. Of course, the safekeeping and uninterrupted flow of such products are of crucial and multifold importance to the industrialized world. In this context, the structures holding these products play an important role to a wide range of industrial facilities, municipalities, environmental agencies, etc.

In most recent works on the subject, as well as in this one, the term sloshing is used for the description of the liquid motion in a partially filled container. It is assumed that the liquid volume is bounded by a free surface at the interface with the gas occupying the remaining of the container. The free surface oscillates at well defined modal shapes and corresponding natural frequencies, which depend on the amount of liquid and, of course, the shape and size of the tank. As a consequence, forced oscillations, at a frequency close to a natural one, will cause resonance phenomena, manifested in the form of large free-surface displacements, which may become detrimental to the integrity of the containing structure.

A simple but accurate and efficient methodology for the estimation of the hydrodynamic pressures exerted on the walls of a tank, which is of prime interest to structural engineering, was proposed in the pioneering works of Housner [2,3]. In these studies on nondeformable vertical tanks of circular or rectangular section resting on rigid foundations, the solution describing the total hydrodynamic pressure was decomposed into two discrete parts: the "impulsive" and the "convective." The impulsive pressure component is due to a portion of the liquid accelerating with the rigid tank, while the convective pressure is exerted by the sloshing motion oscillating at a fundamental frequency. A similar development of an equivalent spring-mass system, replacing the moving fuel in an airplane tank, was also reported by Graham and Rodriguez [4].

In addition to the dynamics of a rigid liquid container, a number of other issues have been studied since these early works. From the structural engineering point of view, the most notable of these are the interaction between the deformable tank walls and the contained liquid, e.g., Veletsos and Yang [5,6], Haroun [7,8], Haroun and Housner [9], and Balendra et al. [10], and the interaction between the supporting medium (soil) and the tank structure, including the uplifting and anchoring effects, e.g., Wozniak and Mitchell [11], Fischer [12], Natsiavas [13], Natsiavas and Babcock [14], Peek [15], Seeber et al. [16], Veletsos and Tang [17], Fischer et al. [18], and Malhotra [19]. This extensive analytic and numerical effort is experimentally supported by the works of, e.g., Clough and Niwa [20], Manos and Clough [21], and Sakai et al. [22]. Almost all of the above mentioned works deal exclusively with vertical prismatic tanks of circular or rectangular section. A more complete list of references on this subject can be found in the review articles of Rammerstorfer and Scharf [23] and Ibrahim et al. [24]. Nevertheless, the "impulsive-convective" pressure concept along with the findings of the above referenced works lie the basis of almost all recent design codes and guidelines, e.g., API Standard 650 [25], Eurocode 8 [26], and ASCE [27].

In comparison to the vast body of publications concerning vertical prismatic tanks, only few works have appeared on other tank geometries. Of those, the most frequently met are the ones dealing with spherical and horizontal cylindrical tanks. Budiansky [28] was apparently the first who studied such structures and obtained numerical solutions using integral equations and 3D transformations. Semi-analytical/numerical solutions have also been reported by Chu [29], Moiseev and Petrov [30], Fox and Kutler [31,32], McIver [33], McIver and McIver [34], Papaspyrou et al. [35–37], and Patkas and Karamanos [38]. Experimental investigations of sloshing in spherical and horizontal cylindrical tanks have been reported by Abramson et al. [39,40] and Kobayashi et al. [41].

Finally, reference is made to numerical solutions obtained by

[1]Corresponding author.

Contributed by the Vessel and Piping Division of ASME for publication in the JOURNAL OF PRESSURE VESSEL TECHNOLOGY. Manuscript received October 31, 2006; final manuscript received May 16, 2007; published online September 10, 2008. Review conducted by F. W. Brust.

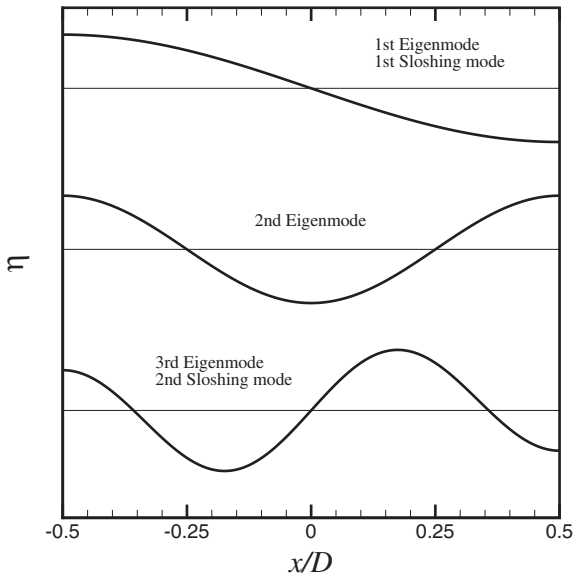

Fig. 1 Typical free-surface shapes η, for the first three eigenmodes, of liquid motion in vertically axisymmetric storage tanks under horizontal seismic excitation in the *x* direction. *D* is the tank diameter at the free surface when the liquid is at rest.

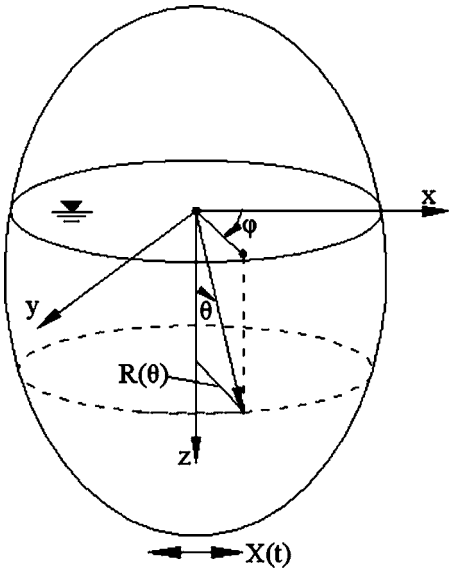

Fig. 3 Coordinate system for axisymmetric (with respect to *z*) storage tanks

the application of the most popular, in recent times, numerical methods, i.e., the finite element method (FEM) and the boundary element method (BEM), since they provide the means for the solution of complicated geometries, boundary conditions, and couplings between the liquid and solid domains. Among the various applications of the FEM one can mention the classic works of Balendra et al. [42] and Haroun [43], and the most recent of Karamanos et al. [44], where the entire liquid volume is discretized by two—or three-dimensional elements, depending on the type of the problem. The BEM offers a computationally less intensive solution since for certain linearized problems, only the free surface of the liquid domain is discretized, e.g., Dutta and Laha [45]. However, the efficient coupling of the two methods seems to provide a computationally attractive alternative for the most demanding fluid-structure interaction problems, e.g., Hwang and Ting [46] and Koh et al. [47]. A comprehensive discussion and literature review on these matters can be found in Ref. [48].

A detailed search through the available literature reveals that the impulsive-convective pressure concept is almost universally accepted as the solution of choice for the analysis and design of vertical prismatic tanks of cylindrical and rectangular cross sections. However, very little information exists regarding the application of this concept to tanks of other geometries. In addition, the distribution of the hydrodynamic pressure on the walls of tanks of nonprismatic geometry is almost completely missing. This is mainly due to the fact that, so far, the development of discrete impulsive-convective spring-mass systems is, in most cases, based on analytical solutions. This precludes the development of such simple solutions for more complicated geometries and boundary conditions. Therefore, this work aims at establishing a simple yet accurate numerical methodology for the computation of the impulsive-convective mass system that can be used in the seismic design of liquid containers of arbitrary shape and fill height. To this end, an eigenmode analysis is used in conjunction with a simple but elegant fluid model, which is readily accessible through most of the commercially available general purpose FEM programs, e.g., ANSYS [49]. Even though a FEM analysis can handle a variety of complicated fluid and structural models, as well as their various interactions, in an effort to concentrate on the influence of the geometry and to illustrate the generality of the proposed methodology, the fluid flow model used in this work is

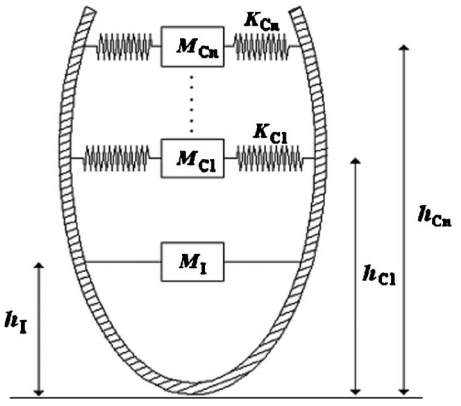

Fig. 2 Model for the representation of fluid motion in liquid storage tanks by discrete masses and spring

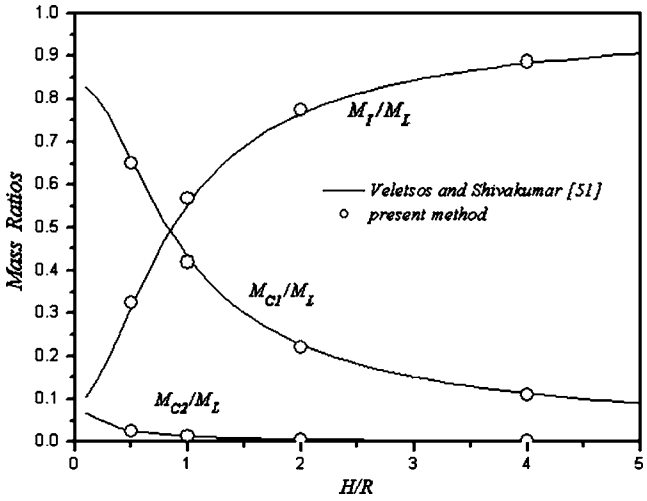

Fig. 4 Convective and impulsive mass variations versus the dimensionless fill height for vertical cylindrical tanks

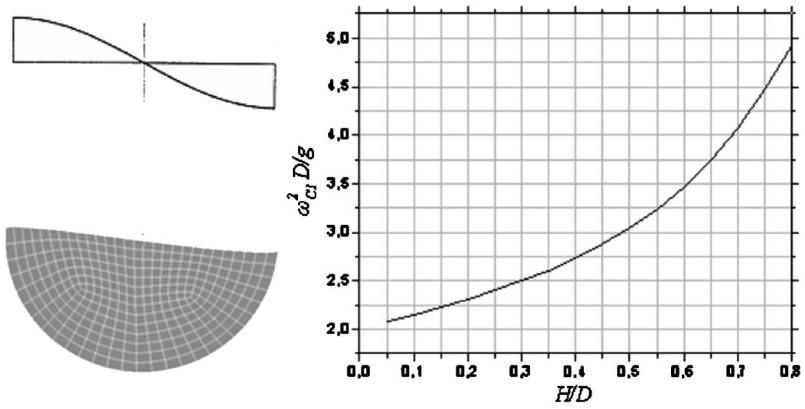

Fig. 5 First sloshing mode of spherical tanks: the free surface and mode shape of half-full case (left) and the variation of the dimensionless frequency versus the dimensionless fill height (right)

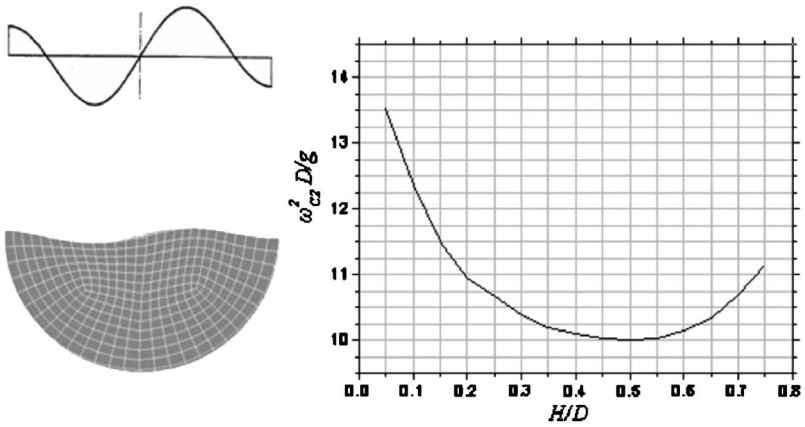

Fig. 6 Second sloshing mode of spherical tanks: the free surface and the mode shape of the half-full case (left) and the variation of the dimensionless frequency versus the dimensionless fill height (right)

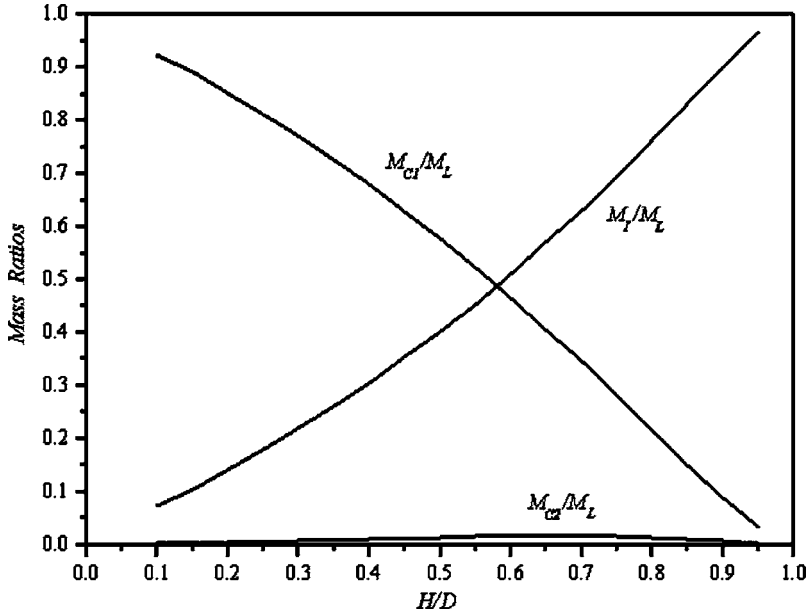

Fig. 7 Convective and impulsive mass variations versus the dimensionless fill height for spherical tanks

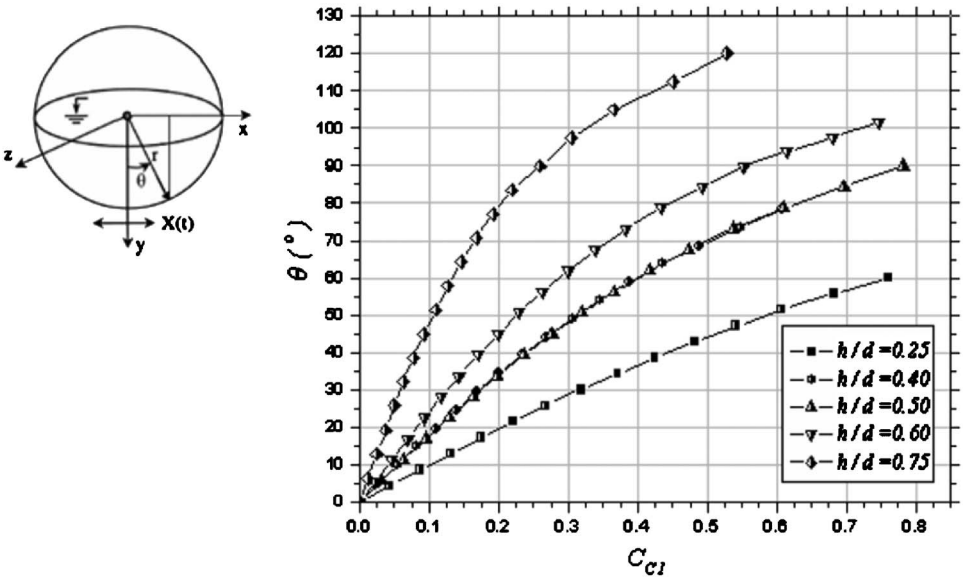

Fig. 8 Convective pressure profile variation with the azimuthal angle for several fill heights in spherical tanks

linear (small free-surface amplitude) and inviscid (slip wall condition), while the tank walls are assumed rigid. In Sec. 3 applications of the proposed methodology are shown for vertical cylindrical, spherical, and conical tanks. The accuracy, computational efficiency, and versatility of the proposed methodology are demonstrated through comparison studies with results available in literature.

2 Numerical Formulation

The eigenmode-based formulation of sloshing in a tank of arbitrary shape and fill height, under horizontal excitation, results into the computation of the eigenmode frequencies, the convective-impulsive mass decomposition, and the corresponding distribution of wall pressures. The fluid flow is considered to be inviscid (slip wall condition) and linear (small free-surface steepness). The numerical solution presented in this work is based on a finite element model developed within the environment provided by the ANSYS [49] software.

FEM Fluid Model. The bulk motion of the liquid is modeled using the lumped mass matrix method while assuming isotropic material properties, with the elastic modulus being equal to the bulk modulus of the liquid. Thus, the stress-strain relationship used for the development of the appropriate stiffness matrix of the fluid element is

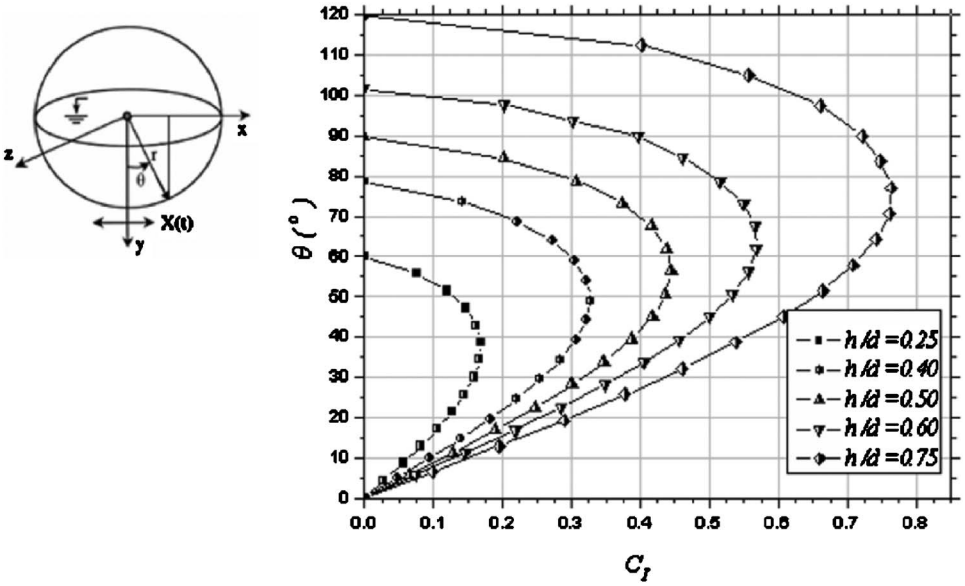

Fig. 9 Impulsive pressure profile variation with the azimuthal angle for several fill heights in spherical tanks

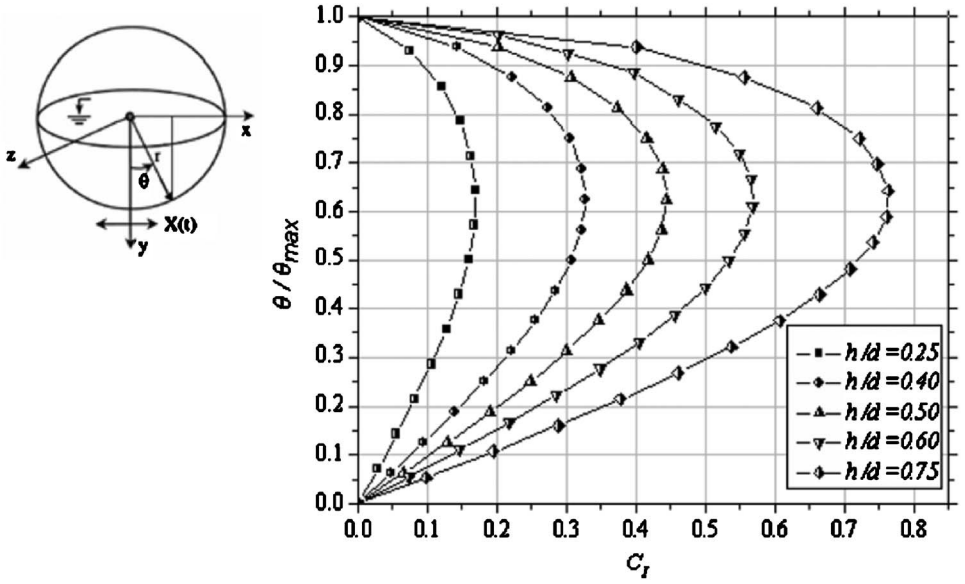

Fig. 10 Impulsive pressure profile variation with the normalized azimuthal angle for several fill heights in spherical tanks

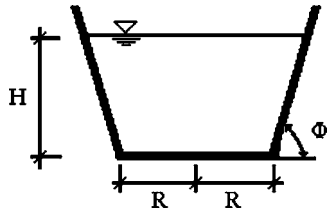

Fig. 11 Geometry and nomenclature of conical tanks

$$\begin{Bmatrix} \varepsilon_{\text{bulk}} \\ \gamma_{xy} \\ \gamma_{yz} \\ \gamma_{zx} \\ \vartheta_x \\ \vartheta_y \\ \vartheta_z \end{Bmatrix} = \begin{bmatrix} \frac{1}{K} & 0 & 0 & 0 & 0 & 0 & 0 \\ 0 & \frac{1}{S} & 0 & 0 & 0 & 0 & 0 \\ 0 & 0 & \frac{1}{S} & 0 & 0 & 0 & 0 \\ 0 & 0 & 0 & \frac{1}{S} & 0 & 0 & 0 \\ 0 & 0 & 0 & 0 & \frac{1}{B} & 0 & 0 \\ 0 & 0 & 0 & 0 & 0 & \frac{1}{B} & 0 \\ 0 & 0 & 0 & 0 & 0 & 0 & \frac{1}{B} \end{bmatrix} \begin{Bmatrix} P \\ \tau_{xy} \\ \tau_{yz} \\ \tau_{zx} \\ M_x \\ M_y \\ M_z \end{Bmatrix} \tag{1}$$

where $\varepsilon_{\text{bulk}} = (\partial u/\partial x) + (\partial v/\partial y) + (\partial w/\partial z)$ is the volumetric strain, with u, v, and w being the displacements along the axes of the

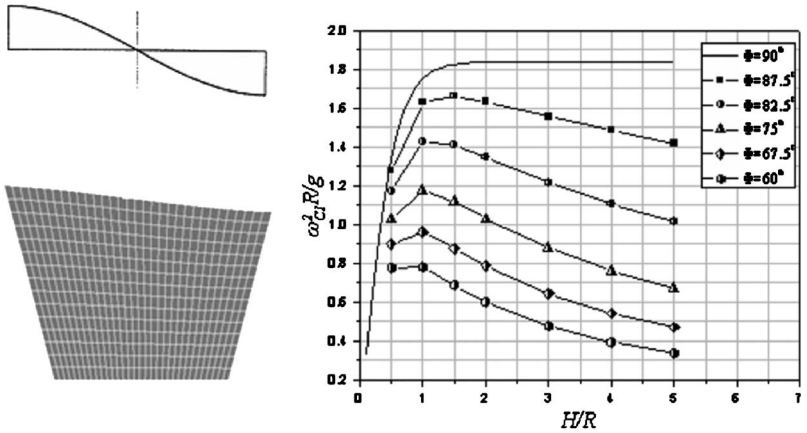

Fig. 12 First sloshing mode of conical tanks: the typical free surface and the mode shape (left) and the frequency variation with the dimensionless fill height and the tank wall angle Φ (right)

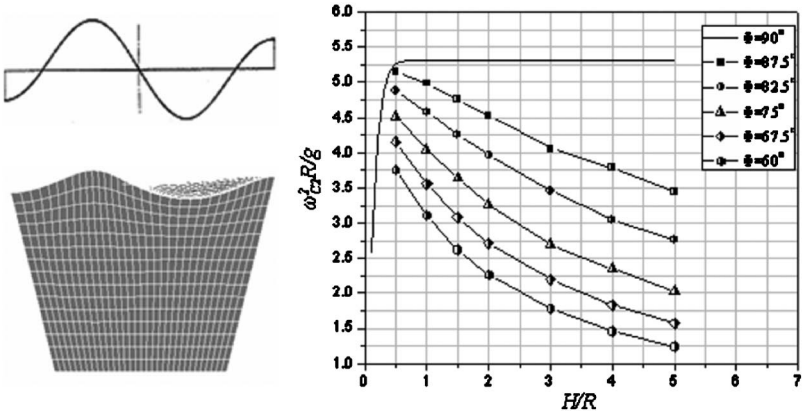

Fig. 13 Second sloshing mode of conical tanks: the typical free surface and the mode shape (left) and the frequency variation with the dimensionless fill height and the tank wall angle Φ (right)

Cartesian coordinate system x, y, and z respectively, K is the bulk modulus, P is the pressure, γ_{ij} and τ_{ij} are the shear strains and stresses, and ϑ_i and M_i are the rotations and corresponding moments. The parameters S and B are used only for stability in the shear and torsion and assume arbitrarily small values of the order of $K\times 10^{-9}$. Using Eq. (1) and following standard FEM procedures, e.g., Ref. [50], results to the development of a 3D element, which can simulate the behavior of a linear elastic isotropic material defined only by its bulk modulus. Such an element with eight nodes and three translational degrees-of-freedom per node is employed in this work [49].

The motion of the liquid free surface is modeled with additional (fictitious) vertical spring elements, which are attached to the nodal points located on the free surface. The stiffness $(K_{\mathrm{fs}})_i$ of the linear spring attached to node i is computed as

$$(K_{\mathrm{fs}})_i = \rho g A_i \tag{2}$$

where ρ is the liquid density, g is the acceleration of gravity, and A_i is the area of free surface, which corresponds to node i. Normal to the rigid tank wall, a zero relative displacement condition is enforced, which is equivalent to the slip boundary condition of inviscid fluid motion.

Based on the above assumptions and an appropriate discretization of the entire fluid volume, the mass $[M]$ and stiffness $[K]$ matrices are assembled following standard FEM procedures. Subsequently, a modal analysis can be performed using anyone of the well known eigenvalue extraction algorithms, e.g., full or reduced [50]. In any case, for each eigenmode, the computation of the eigenfrequency ω_i and the corresponding eigenvector $\{\phi\}_i$ is based on the solution of the equation

$$[[K] - \omega_n^2[M]]\{\phi\}_n = 0 \tag{3}$$

where $n=1,2,\ldots,3N$, with N being the total number of nodal points. However, it should be noted that only those modes corresponding to a vertical motion of the free surface are of interest and are retained for further analysis. Thus, eigenvalue/eigenvector extraction procedures, operating on appropriately condensed systems of equations, present obvious computational advantages for the solution of the problems studied in this work.

Discrete Convective-Impulsive Model. The total hydrodynamic pressure applied on the tank walls during a horizontal seismic excitation can be decomposed into an impulsive part, which is associated with the fluid motion that has zero relative acceleration with respect to the tank motion, and a convective part, which is associated with the fluid sloshing motion. Similarly, the total horizontal force applied on the tank due to the fluid motion can be decomposed into an impulsive and a convective component.

The sloshing motion can be represented as a superposition of some appropriate eigenmodes of the fluid motion. In general, each eigenmode generates a hydrodynamic wall pressure of unique distribution, but not all of these modes contribute to the development of a nonzero horizontal force on the tank. For example, for a vertically axisymmetric tank, such as a cylindrical or a spherical one, the eigenmodes, which are responsible for the generation of a nonzero horizontal hydrodynamic force and, thus, influence the horizontal motion of the tank structure, are those that exhibit free-surface antisymmetry with respect to a plane that is parallel to the tank axis of symmetry. These eigenmodes are called sloshing modes. Typical free-surface profiles of the first three eigenmodes, for a vertically axisymmetric tank, are shown in Fig. 1. According to the above discussion, the first eigenmode corresponds to the first sloshing mode and the third eigenmode corresponds to the second sloshing mode, while the second eigenmode does not contribute to the development of a horizontal force. The discrete masses M_{Cn}, associated with the sloshing modes $n=1,\ldots,\infty$, are called convective. The convective masses and the impulsive mass M_I, i.e., the remaining portion of the total mass moving in synchronism with the tank, are related via the principle of conservation of mass as

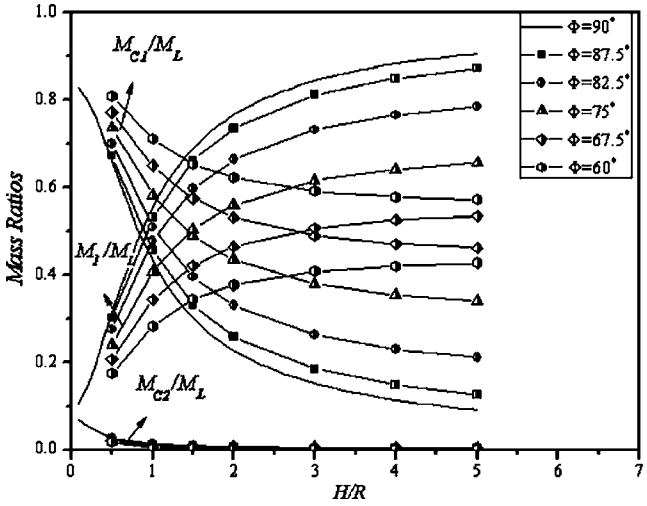

Fig. 14 Convective and impulsive mass variations with the dimensionless fill height and the tank wall angle Φ for conical tanks

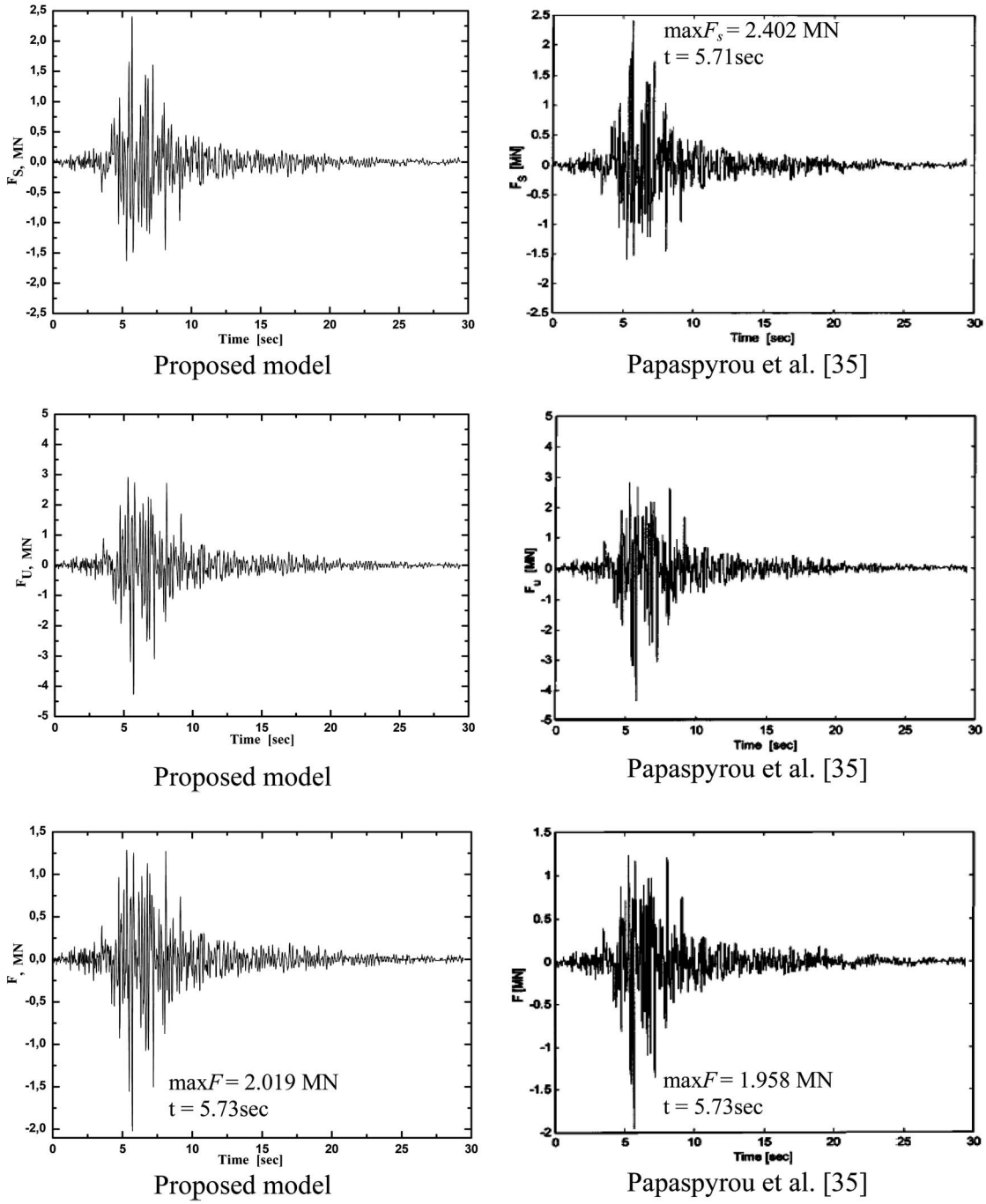

Fig. 15 Time histories of convective, impulsive, and total hydrodynamic forces on a spherical tank subject to the Kozani seismic excitation

$$M_L = M_I + \sum_{n=1}^{\infty} M_{\mathrm{Cn}} \tag{4}$$

$$F(t) = M_I \ddot{x}(t) - \sum_{n=1}^{\infty} M_{\mathrm{Cn}} \omega_n^2 u_n(t) \tag{5}$$

where M_L stands for the entire liquid mass.

Following the above discussion on the convective-impulsive decomposition, the instantaneous value of the total horizontal hydrodynamic force or base shear, F, applied on the tank due to the liquid motion, can be computed, e.g., Ref. [51], as

where $\ddot{x}(t)$ is the acceleration of the tank structure and $u_n(t)$ is the response of a single degree-of-freedom system with frequency ω_n, which is computed using as forcing input the acceleration of the tank.

Although for vertical or horizontal cylindrical and spherical tanks the computation of the impulsive and convective masses,

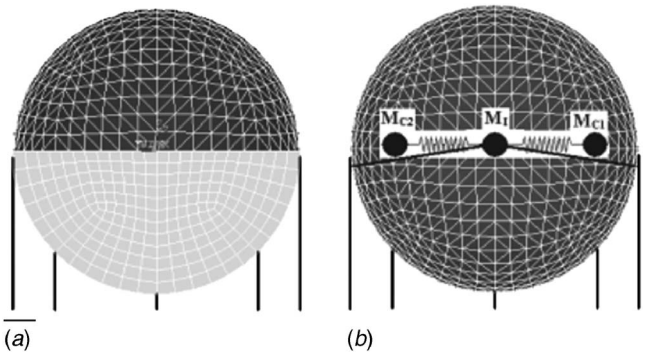

Fig. 16 (*a*) Full FEM and (*b*) hybrid models of a spherical tank supported by a series of columns

involved in Eqs. (4) and (5), is available in analytical or semi-analytical form, e.g., Refs. [35,36,51], this is not the case for tanks of arbitrary shapes. Apparently, their computation for arbitrary tank shapes is a critical step toward the development of a discrete system for such a structure. Toward this end, the concept of an oscillator with multiple degrees-of-freedom is employed in this work, in view of the form of Eq. (5). Therefore, the convective mass M_{Cn} of each sloshing mode is equal to an effective (equivalent) modal mass computed according to, e.g., Chopra [52],

$$M_{\mathrm{Cn}} = \frac{(L_{\mathrm{Cn}})^2}{M_n} \tag{6}$$

where $M_n = \{\phi\}_n^T[M]\{\phi\}_n$ is the normal-coordinate generalized mass of eigenmode n, $L_{\mathrm{Cn}} = \{\phi\}_n^T[M]\{I\}$, and $\{I\}$ is a vector of unit length in the direction of the seismic excitation.

As mentioned above, the convective-impulsive mass decomposition results into the representation of the dynamic behavior of the hydrodynamic force due to sloshing by an equivalent system of discrete masses and springs. A schematic representation of such a system, for a tank of arbitrary shape under horizontal seismic excitation, is shown in Fig. 2 where the convective portion of the liquid is substituted by an equivalent system of masses and springs, while the impulsive portion reduces to a single mass rigidly connected to the tank wall. On the basis of the previous discussion and derivations, the spring constants for each convective mass can be calculated as

$$K_{\mathrm{Cn}} = \omega_n^2 M_{\mathrm{Cn}} \tag{7}$$

The position height, h_{Cn} or h_I, of each mass depends on the convective-impulsive pressure distribution on the tank wall, considering the fact that the fluid pressure generates a stress normal to the tank wall. For vertical prismatic tanks the position heights are available in analytic form, e.g., Refs. [2,3,24]. For a spherical tank or a horizontal cylinder of diameter D, all discrete masses should be placed at the geometrical center, i.e., $h_{\mathrm{Cn}} = h_I = D/2$, since all resultant forces due to the fluid pressure are applied at the geometrical center of the container. For arbitrary tank geometries, the corresponding heights can be calculated via a straightforward numerical integration of the fluid pressure distribution and a subsequent positioning of the resultant force using standard procedures, e.g., Ref. [51].

Similarly, the total hydrodynamic pressure distribution on the tank wall can be decomposed, in general, into an impulsive part, which is associated with the fluid motion that has zero relative acceleration with respect to the tank motion, a convective part, which is associated with the fluid sloshing motion, and an axisymmetric part, which is associated with the axisymmetric eigenmodes of the fluid motion that do not contribute to the total horizontal force. The pressure decomposition is

$$p(\theta,\varphi,t) = p_I(\theta,\varphi,t) + \sum_{n=1}^{\infty} p_{\mathrm{Cn}}(\theta,\varphi,t) + \sum_{m=1}^{\infty} p_{\mathrm{Am}}(\theta,t) \tag{8}$$

where θ and φ are the azimuth and meridian angles, respectively, as shown in Fig. 3, p_I is the impulsive pressure, p_{Cn} is the convective pressure due to sloshing mode n, and p_{Am} is the axisymmetric pressure due to axisymmetric mode m. For vertically axisymmetric tanks under horizontal seismic excitation, only the sloshing modes are excited; therefore, the axisymmetric pressure is zero. Then, the impulsive pressure is given by the expression

$$p_I(\theta,\varphi,t) = C_I(\theta)\rho R(\theta)\cos(\varphi)\ddot{x}(t) \tag{9}$$

while the convective pressure for each sloshing mode is given by the expression

$$p_{\mathrm{Cn}}(\theta,\varphi,t) = -C_{\mathrm{Cn}}(\theta)\omega_n^2\rho R(\theta)\cos(\varphi)u_n(t) \tag{10}$$

with C_I and C_{Cn} being dimensionless pressure profile functions, which depend on the tank fill height.

The computation of the convective pressure profile functions is based on a series of dynamic mode superposition analyses. Thus, for any fill height, the response of the fluid-structure FEM model to an arbitrary seismic excitation is computed taking into consideration only the nth sloshing mode computed from Eq. (3). The resulting hydrodynamic pressure distribution is equal to p_{Cn}, and, therefore, the profile functions C_{Cn} can be computed using Eq. (10). Then, a time simulation is performed, based on the same seismic excitation as in the dynamic mode superposition analysis, and the total hydrodynamic pressure distribution p is obtained. Finally, the impulsive pressure distribution p_I results from Eq. (8) and the corresponding pressure profile function C_I from Eq. (9).

3 Validation and Numerical Applications

In this section, the methodology described in the previous section is applied to vertical cylindrical tanks, spherical tanks, and conical tanks. Parametric studies have been contacted for the optimization of the finite element mess and, finally, the results presented are based on a resolution of about 50 nodes per tank diameter (base diameter for the conical tanks). All the numerical results, unless otherwise indicated, pertain to a bulk modulus of $K = 2.19 \times 10^6$ kPa (water) for the liquid domain.

Sloshing Frequencies, Convective-Impulsive Masses, and Hydrodynamic Pressure. As mentioned earlier, the case of vertical cylindrical tanks with rigid walls has appeared frequently in literature and, for this reason, is used here for validation purposes. A comparative study of the results obtained by the proposed methodology and those reported by Veletsos and Shivakumar [51] is attempted in Fig. 4, where the ratios of the discrete impulsive M_I and convective M_{Cn} masses to the total liquid mass M_L are plotted versus the ratio H/R, where H is the liquid height and R is the tank radius. Apparently, there is virtual coincidence of the results obtained by the two methods for the entire range of H/R values. It is noted that since higher sloshing modes have a relatively negligible impact on the results, only the first two sloshing modes are used in Eq. (4) for the calculation of the impulsive mass.

Next, the case of spherical tanks is presented. The variation of the eigenfrequencies of the first two sloshing modes versus the dimensionless ratio H/D of liquid height H (measured from the south pole of the tank) to sphere diameter D is shown in Figs. 5 and 6. For the first sloshing mode, the eigenfrequency increases monotonically with the increase in H/D, while for the second sloshing mode, the corresponding eigenfrequency exhibits a local minimum for $H/D = 0.5$. The variation of ratios M_{Cn}/M_L and M_I/M_L versus H/D is shown in Fig. 7. It is apparent, as for vertical cylindrical tanks, that only the first two sloshing modes have any significant impact on the sloshing motion, with the first being dominant for all practical purposes. It is also worth noting the prominence of the convective mass at lower fill heights while

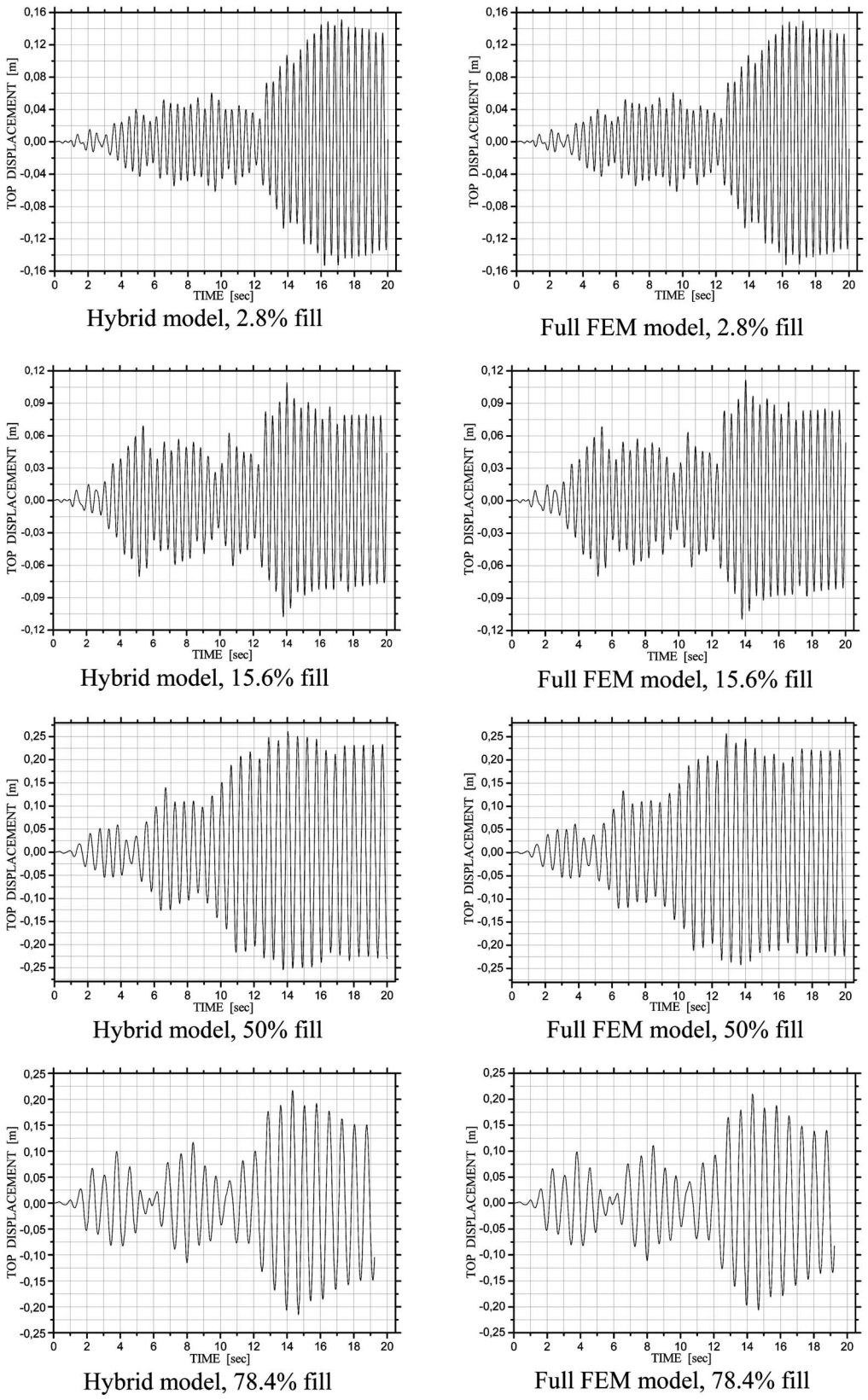

Fig. 17 Time histories of the horizontal displacement at the north-pole of the spherical tank subject to an artificial accelerogram compatible to EC8 for several fill ratios and comparison of results obtained by the full FEM and the hybrid models in Fig. 16

the reverse is true at higher fill levels. At approximately $H/D = 0.58$ the convective and impulsive masses become equal. The variation of the convective pressure profile C_{C1} of the first sloshing mode and the impulsive pressure profile C_I versus θ, for sev-

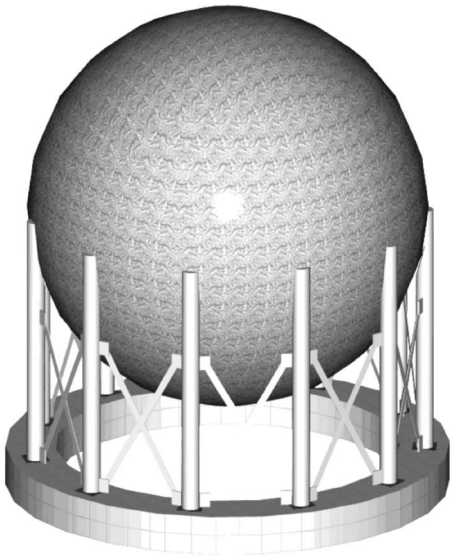

Fig. 18 Spherical tank supported by a series of columns and tension-only diagonal braces

eral values of H/D, are shown in Figs. 8 and 9, respectively. The impulsive pressure profile C_I versus the normalized angle $\theta/\theta_{\max}$ is shown in Fig. 10, where it is demonstrated that the maximum impulsive pressure manifests at a constant value of $\theta/\theta_{\max}=0.63$.

The geometry of conical tanks is shown in Fig. 11. The eigenfrequency variation versus the ratio H/R, with H being the liquid height and R being the base radius, for the first two sloshing modes and several values of the sidewall angle (Φ) is shown in Figs. 12 and 13. The case $\Phi=90$ deg corresponds to a vertical cylindrical tank. For both sloshing modes and $\Phi<90$ deg, the eigenfrequency exhibits a local maximum at a critical value (H/R) and decreases with increasing $H/R>(H/R)_{\text{cr}}$. For the first sloshing mode, the value of $(H/R)_{\text{cr}}$ decreases from a value of 1.5 for $\Phi=87.5$ deg to 0.75 for $\Phi=60$ deg. For the second sloshing mode, the corresponding $(H/R)_{\text{cr}}$ values are smaller than that of the first mode. The variation of ratios M_{Cn}/M_L and M_I/M_L versus H/R for several values of the sidewall angle Φ is shown in Fig. 14. Decreasing the angle Φ results, as it was expected, into a reduction in the impulsive mass and an increase in the convective ones. Again, it is apparent that only the first two sloshing modes have any significant impact on the sloshing motion.

Seismic Response of Spherical Tanks. Three examples are presented in order to demonstrate the effectiveness and accuracy of the proposed discrete model for the simulation of sloshing motion in liquid storage tanks. They pertain to the seismic response of spherical tanks, where the results computed by the proposed discrete model are compared to those obtained using detailed fluid discretizations.

First, the seismic response of a simple rigid spherical tank is considered. The tank has diameter $D=20$ m and is half-full with a liquid of density $\rho=1000$ kg/m^3. The seismic excitation considered is the horizontal record of Kozani obtained from the European Strong Motion Database.[2] A discrete mass model is utilized where the liquid is replaced by the first two convective masses and the impulsive mass. The total liquid mass is $M_L=2094.4$ ton, while the convective masses are computed, utilizing Fig. 7, as $M_{C1}=0.5745\cdot M_L=1203.2$ ton and $M_{C2}=0.0135\cdot M_L=28.3$ ton. The impulsive mass is $M_I=M_L-M_{C1}-M_{C2}=862.9$ ton. All masses are attached to the center of the sphere, while the spring constants of the convective masses are computed by Eq. (7) and

[2]www.isesd.cv.ic.ac.uk.

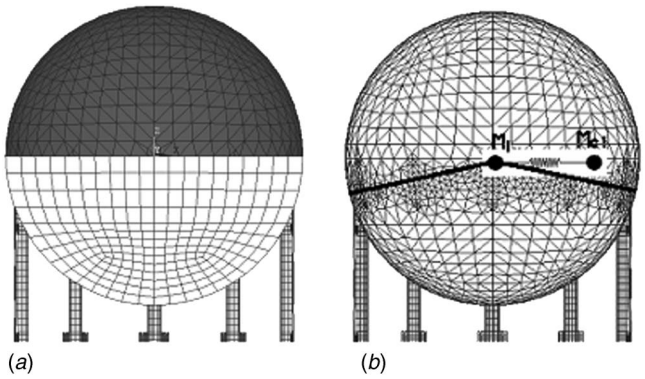

Fig. 19 (*a*) Full FEM and (*b*) hybrid models of the spherical tank in Fig. 18

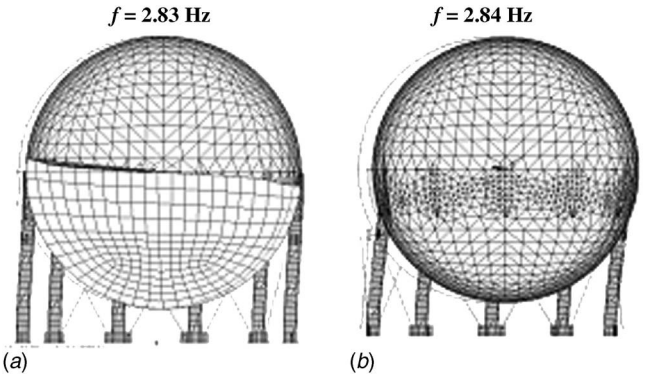

Fig. 20 Shape and frequency of the first eigenmode obtained by the full FEM and the hybrid models in Fig. 19

Figs. 5 and 6. The time history of the base shear force due to sloshing F_S, impulsive F_I, and the total force hydrodynamic force F exerted on the tank is shown in Fig. 15. The results obtained by the proposed discrete model are in excellent agreement to those reported by Papaspyrou et al. [35].

Next, the seismic response of a rigid spherical tank supported by a series of columns (simple beam elements), as shown in Fig. 16, is examined. The tank has a diameter of $D=20$ m and the density of the contained liquid is $\rho=522$ kg/m^3. Several fill height ratios are considered. The tank is subject to an artificial seismic excitation compatible to the design seismic spectra of EC8. The response of the tank is simulated considering (a) a full FEM model for the structure and the fluid and (b) a hybrid model where the same FEM model, as in (a), is maintained for the structure while the liquid motion is represented by a discrete model, as proposed in this work, with two convective and the impulsive masses, as shown in Fig. 16. The impulsive mass is located at the center of the sphere and is attached to the spherical shell by a series of rigid links, which are connected to the column-shell intersection. The convective masses are connected to the center of the sphere via convective springs, as shown in Fig. 16(*b*). The discrete masses and the spring constants are calculated from the charts of Figs. 5–7 and Eq. (7). For every fill height ratio, the convective masses are computed utilizing Fig. 7. All masses are attached to the center of the sphere, while the spring constants of the convective masses are computed by Eq. (7) and Figs. 5 and 6. The time histories of the horizontal displacement of the tank north-pole are shown in Fig. 17. Apparently, the results computed by the two models are in excellent agreement.

Finally, the seismic response of the deformable spherical tank shown in Fig. 18 is examined. The tank has a diameter of D

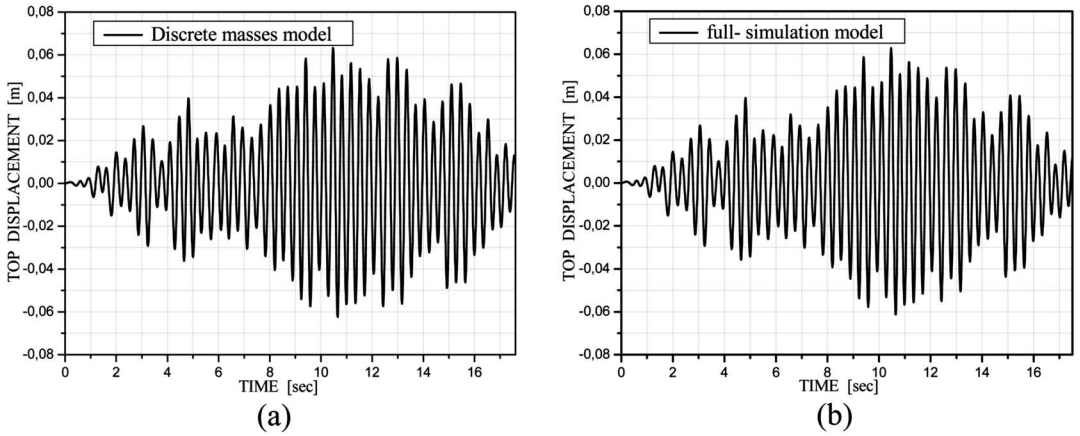

Fig. 21 Time histories of the horizontal displacement at the north-pole of a half-full spherical tank subject to an artificial accelerogram compatible to EC8 and comparison of results obtained by the full FEM and the hybrid models in Fig. 19

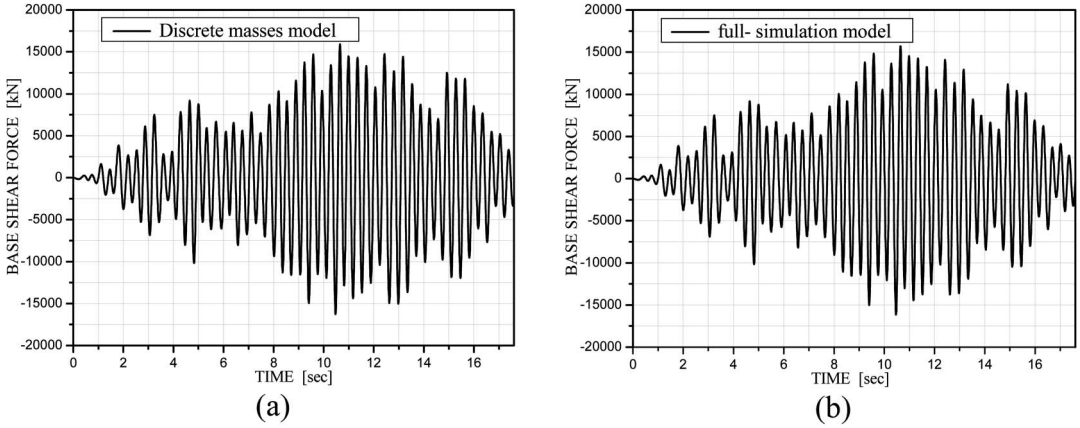

Fig. 22 Time histories of the base shear force of a half-full spherical tank subject to an artificial accelerogram compatible to EC8 and comparison of results obtained by the full FEM and the hybrid models in Fig. 19

=20 m and is half-full with a liquid of density $\rho=522$ kg/m^3. The tank, a complete description of which can be found in Ref. [53], is supported on a series of cylindrical columns and its horizontal motion is restrained by a set of diagonal braces, which are assumed to work only in tension. The tank is subject to an artificial seismic excitation compatible to the design seismic spectra of EC8, for soil Type C and PGA=0.4 g. As in the previous example, the response of the tank is simulated considering (a) a full FEM model for the structure and the fluid and (b) a hybrid model where the same FEM model, as in (a), is maintained for the structure while the liquid motion is represented by a discrete model with two masses (one convective and one impulsive), as shown in Fig. 19. The convective mass is attached to the impulsive mass located at the center of the sphere via a spring element. The impulsive mass is connected to the spherical shell by rigid links, which are attached to the geometrical center of the column-spherical shell connection. The total liquid mass is M_L =1093.3 ton. The first convective mass obtained from Fig. 7, is $M_{C1}=0.5745\cdot M_L=628.1$ ton, while the impulsive mass is M_I $=M_L-M_{C1}=465.2$ ton. The spring constant of the convective mass is $K_{C1}=939.5$ kN/m as computed by Eq. (7) and Fig. 5 where $\omega_{C1}^2 D/g=3.05$. The shape and the frequency of the first eigenmode of the tank motion are shown in Fig. 20. The time histories of the horizontal displacement at the north-pole and the total base shear force are shown in Figs. 21 and 22, respectively. For all these results, the predictions of the hybrid model are in excellent agreement to those of the full FEM simulation. However, it should be noticed that while only two discrete masses and one spring element are necessary for the representation of the sloshing liquid using the proposed model, a total of 3000 finite elements (ANSYS, FLUID80) is used in the full FEM model.

4 Conclusions

A simple but computationally effective model has been proposed for the simulation of sloshing liquids in tanks of arbitrary shape. The methodology for the computation of the convective and impulsive masses and the associated spring constants is based on standard FEM analyses available in almost all commercially available finite element software. The results obtained by the proposed methodology for cylindrical and spherical tanks are in excellent agreement to those already available in literature. In addition, results for conical tanks are presented. Seismic analyses of elevated spherical tanks simulating realistic structures reveal the computational efficiency and accuracy of the proposed models. Obviously, the use of the proposed discrete models results in a dramatic reduction in the size of the dynamic model. Thus, it can become a useful tool for quick yet accurate analyses in the design office.

References

[1] Lamb, H., 1932, *Hydrodynamics*, Cambridge University Press, Cambridge.

[2] Housner, G. W., 1957, "Dynamic Pressures on Accelerated Fluid Containers," Bull. Seismol. Soc. Am., **47**, pp. 15–35.
[3] Housner, G. W., 1963, "The Dynamic Behavior of Water Tanks," Bull. Seismol. Soc. Am., **53**, pp. 381–387.
[4] Graham, E. W., and Rodriguez, A. M., 1952, "The Characteristics of Fuel Motion Which Affect Airplane Dynamics," ASME J. Appl. Mech., **19**, pp. 381–388.
[5] Veletsos, A. S., and Yang, J. Y., 1976, "Dynamics of Fixed-Base Liquid Storage Tanks," *US-Japan Seminar for Earthquake Engineering Research*, Tokyo, Japan, pp. 317–341.
[6] Veletsos, A. S., and Yang, J. Y., 1977, "Earthquake Response of Liquid Storage Tanks," *Proceedings of the Second EMD Specialty Conference (ASCE)*, Raleigh, NC, pp. 1–24.
[7] Haroun, M. A., 1980, "Dynamic Analyses of Liquid Storage Tanks," California Institute of Technology, Report No. EERL 80-04.
[8] Haroun, M. A., 1983, "Vibration Studies and Tests of Liquid Storage Tanks," Earthquake Eng. Struct. Dyn., **11**, pp. 179–206.
[9] Haroun, M. A., and Housner, G. W., 1981, "Seismic Design of Liquid Storage Tanks," J. Technical Councils of ASCE, **107**, pp. 191–207.
[10] Balendra, T., Ang, K. K., Paramasivam, P., and Lee, S. V., 1982, "Seismic Design of Flexible Cylindrical Liquid Storage Tanks," Earthquake Eng. Struct. Dyn., **10**, pp. 477–496.
[11] Wozniak, R. S., and Mitchell, W. W., 1978, "Basis of Seismic Design Provisions for Welded Steel Oil Storage Tanks," *Proceedings of the Session on Advances in Storage Tank Design*, API Refining Department, Toronto, Canada, pp. 485–493.
[12] Fischer, F. D., 1979, "Dynamic Fluid Effects in Liquid-Filled Flexible Cylindrical Tanks," Earthquake Eng. Struct. Dyn., **7**, pp. 587–601.
[13] Natsiavas, S., 1988, "An Analytical Model for Unanchored Fluid-Filled Tanks Under Base Excitation," ASME J. Appl. Mech., **55**, pp. 648–653.
[14] Natsiavas, S., and Babcock, C. D., 1988, "Behavior of Unanchored Fluid-Filled Tanks Subjected to Ground Excitation," ASME J. Appl. Mech., **55**, pp. 654–659.
[15] Peek, R., 1988, "Analysis of Unanchored Liquid Storage Tanks Under Lateral Loads," Earthquake Eng. Struct. Dyn., **16**, pp. 1087–1100.
[16] Seeber, R., Fischer, F. D., and Rammerstorfer, F. G., 1990, "Analysis of a Three-Dimensional Tank-Liquid-Soil Interaction Problem," ASME J. Pressure Vessel Technol., **112**, pp. 28–33.
[17] Veletsos, A. S., and Tang, Y., 1990, "Soil-Structure Interaction Effects for Laterally Excited Liquid Storage Tanks," Earthquake Eng. Struct. Dyn., **19**, pp. 473–496.
[18] Fischer, F. D., Rammerstorfer, F. G., and Scharf, K., 1991, "Earthquake Resistant Design of Anchored and Unanchored Liquid Storage Tanks Under Three-Dimensional Earthquake Excitation," *Structural Dynamics-Recent Advances*, G. I. Schueller, ed., Springer, Berlin, pp. 317–371.
[19] Malhotra, P. K., 1995, "Base Uplifting Analysis of Flexibly Supported Liquid-Storage Tanks," Earthquake Eng. Struct. Dyn., **24**, pp. 1591–1607.
[20] Clough, R. W., and Niwa, A., 1979, "Static Tilt Test of a Tall Cylindrical Liquid Storage Tank," University of California, Report No. UCB/EERC-79/06.
[21] Manos, G. C., and Clough, R. W., 1982, "Further Study of the Earthquake Response of a Broad Cylindrical Liquid-Storage Tank Model," University of California, Report No UCB/EERC-82/7.
[22] Sakai, F., Isoe, A., Hirakawa, H., and Mentani, Y., 1988, "Experimental Study on Uplifting Behavior of Flat-Based Liquid Storage Tanks Without Anchors," *Proceedings of the Ninth World Conference on Earthquake Engineering*, Tokyo/Kyoto, Japan, August 2–9, Vol. VI, pp. 649–654.
[23] Rammerstorfer, F. G., and Scharf, K., 1990, "Storage Tanks Under Earthquake Loading," Appl. Mech. Rev., **43**, pp. 261–282.
[24] Ibrahim, R. A., Pilipchuk, V. N., and Ikeda, T., 2001, "Recent Advances in Liquid Sloshing Dynamics," Appl. Mech. Rev., **54**, pp. 133–177.
[25] American Petroleum Institute, 1995, "Seismic Design of Storage Tanks—Appendix E: Welded Steel Tanks for Oil Storage (API Standard 650)," Washington, DC.
[26] Comité Européen de Normalization, 1998, "Eurocode, 8, Part 4: Silos, Tanks and Pipelines (Annex A)," CEN ENV-1998-4.
[27] ASCE Committee on Gas and Liquid Fuel Lifelines (Technical Council on Lifeline Earthquake Engineering), 1984, "Guidelines for the Seismic Design of Oil and Gas Pipeline Systems," New York.
[28] Budiansky, B., 1960, "Sloshing of Liquids in Circular Canals and Spherical Tanks," J. Aerosp. Sci., **27**, pp. 161–173.
[29] Chu, W.-H., 1964, "Fuel Sloshing in a Spherical Tank Filled to an Arbitrary Depth," AIAA J., **2**, pp. 1972–1979.
[30] Moiseev, N. N., and Petrov, A. A., 1966, "The Calculation of Free Oscillations of a Liquid in a Motionless Container," AIAA J., **9**, pp. 91–154.
[31] Fox, D. W., and Kutler, J. R., 1981, "Upper and Lower Bounds for Sloshing Frequencies by Intermediate Problems," Journal of Applied Mathematics and Physics, **32**, pp. 667–682.
[32] Fox, D. W., and Kutler, J. R., 1983, "Sloshing Frequencies," Journal of Applied Mathematics and Physics, **34**, pp. 669–696.
[33] McIver, P., 1989, "Sloshing Frequencies for Cylindrical and Spherical Containers Filled to an Arbitrary Depth," J. Fluid Mech., **201**, pp. 243–257.
[34] McIver, P., and McIver, M., 1993, "Sloshing Frequencies of Longitudinal Modes for a Liquid Contained in a Trough," J. Fluid Mech., **252**, pp. 525–541.
[35] Papaspyrou, S., Valougeorgis, D., and Karamanos, S. A., 2003, "Refined Solutions of Externally Induced Sloshing in Half-Full Spherical Containers," J. Eng. Mech., **129**, pp. 1369–1379.
[36] Papaspyrou, S., Valougeorgis, D., and Karamanos, S. A., 2004, "Sloshing Effects in Half-Full Horizontal Cylindrical Vessels Under Longitudinal Excitation," ASME J. Appl. Mech., **71**, pp. 255–265.
[37] Papaspyrou, S., Karamanos, S. A., and Valougeorgis, D., 2004, "Response of Half-Full Horizontal Cylinders Under Transverse Excitation," J. Fluids Struct., **19**, pp. 985–1003.
[38] Patkas, L. A., and Karamanos, S. A., 2007, "Variational Solutions of Liquid Sloshing in Horizontal-Cylindrical and Spherical Containers," J. Eng. Mech., **133**, pp. 641–655.
[39] Abramson, H. N., Chu, W.-H., and Garza, L. R., 1963, "Liquid Sloshing in Spherical Tanks," AIAA J., **1**, pp. 384–389.
[40] Abramson, H. N., 1966, "The Dynamic Behavior of Liquids in Moving Containers," Southwest Research Institute, NASA Report No. SP-106.
[41] Kobayashi, N., Mieda, T., Shibata, H., and Shinozaki, Y., 1989, "A Study of the Liquid Slosh Response in Horizontal Cylindrical Tanks," ASME J. Pressure Vessel Technol., **111**, pp. 32–38.
[42] Balendra, T., Ang, K. K., Paramasivam, P., and Lee, S. L., 1982, "Free Vibration Analysis of Cylindrical Liquid Storage Tanks," Int. J. Mech. Sci., **24**, pp. 47–59.
[43] Haroun, M. A., 1983, "Vibration Studies and Tests of Liquid Storage Tanks," Earthquake Eng. Struct. Dyn., **11**, pp. 179–206.
[44] Karamanos, S. A., Patkas, L. A., and Platyrrachos, M. A., 2006, "Sloshing Effects on the Seismic Design of Horizontal-Cylindrical and Spherical Industrial Vessels," ASME J. Pressure Vessel Technol., **128**, pp. 328–340.
[45] Dutta, S., and Laha, M. K., 2000, "Analysis of the Small Amplitude Sloshing of a Liquid in a Rigid Container of Arbitrary Shape Using a Low-Order Boundary Element Method," Int. J. Numer. Methods Eng., **47**, pp. 1633–1648.
[46] Hwang, I. T., and Ting, K., 1987, "Dynamic Analysis of Liquid Storage Tanks Including Hydrodynamic Interaction by Boundary Element Method," *Transactions of the Ninth International Conference on Structural Mechanics in Reactor Technology*, Lausanne, August 17–21, pp. 429–434.
[47] Koh, H. M., Kim, J. A., and Park, J.-H., 1998, "Fluid-Structure Interaction Analysis of 3-D Rectangular Tanks by a Variationally Coupled BEM-FEM and Comparison With Test Results," Earthquake Eng. Struct. Dyn., **27**, pp. 109–124.
[48] Rizos, D. C., and Karabalis, D. L., 2000, "Soil-Fluid-Structure Interaction," *Wave Motion in Earthquake Engineering*, E. Kausel and G. D. Manolis, eds., WIT, Southampton, Chap. 9.
[49] Swanson Analysis Systems, Inc., 1992, "ANSYS, User's Manual for Revision 5.0, Procedures," Houston, PA.
[50] Bathe, K.-J., 1996, *Finite Element Procedures*, Prentice Hall, Englewood Cliffs, NJ.
[51] Veletsos, S. A., and Shivakumar, P., 1984, "Tanks Containing Liquids and Solids," *Computer Analysis and Design of Earthquake Resistant Structures—A Handbook*, D. E. Beskos and S. A. Anagnostopoulos, eds., Computational Mechanics, Southampton.
[52] Chopra, A. K., 1995, *Dynamics of Structures*, Prentice Hall, Upper Saddle River, NJ.
[53] Drosos, J. C., Tsinopoulos, S. V., and Karabalis, D. L., 2005, "Seismic Response of Spherical Liquid Storage Tanks With a Dissipative Bracing System," *Proceedings of the Fifth GRACM International Congress on Computational Mechanics*, Nicosia, Limassol, Cyprus, June 29–July 1, Vol. 1, pp. 313–319.